15 June 2001

ELSEVIER

Optics Communications 193 (2001) 267–276

OPTICS COMMUNICATIONS

www.elsevier.com/locate/optcom

Total internal reflection of spatial solitons at interface formed by a nonlinear saturable and a linear medium

E. Alvarado-Méndez [a,*], R. Rojas-Laguna [a], J.G. Aviña-Cervantes [a], M. Torres-Cisneros [a], J.A. Andrade-Lucio [a], J.C. Pedraza-Ortega [a], E.A. Kuzin [b], J.J. Sánchez-Mondragón [c], V. Vysloukh [c]

[a] *FIMEE Depto. de Electrónica, Universidad de Guanajuato, Apartado Postal 215-A, Salamanca, GTO. 36730, Mexico*
[b] *INAOE, Apartado Postal 51, Puebla, PUE. 7200, Mexico*
[c] *CIICAp Universidad Autónoma del Estado de Morelos, Cuernavaca, Morelos, C.P. 62210, Mexico*

Received 17 February 2000; received in revised form 7 March 2001; accepted 12 April 2001

Abstract

We study numerically and experimentally the reflection of spatial solitons at the interface between a nonlinear saturable-type medium and a linear one. We emphasize on determining the physical conditions under which the reflected beam at the interface conserve its nondiffracting properties. Depending on the incidence angle, we find three critical regions for spatial soliton conservation after reflection. We numerically show that the nonlinear Goos–Hänchen shift can have a dramatic effect on the diffracting properties of the reflected beam. © 2001 Published by Elsevier Science B.V.

PACS: 42.65.Jx; 42.79.Gn

Keywords: Spatial solitons; Photorefractive effect

1. Introduction

The problem of an incidence beam at the interface formed by two nonlinear media of different refractive index, is a fascinating problem from the physical point of view. The reflected beam angle may be controlled easily by varying the power of the input beam, without changing the incident angle of the input beam. This could result in all optical switching devices.

The problem of an interface between a linear and nonlinear Kerr media, in which the incident waves propagate from the linear side, has been previously studied [1–3]. Kaplan [1,2] predicted bistability of the reflection coefficient as a function of the incident intensity. Subsequently, numerical simulations performed by Akhmediev [3] using localized Gaussians beams of finite transverse extent, failed to show bistable reflection. These results confirmed the existence of stable and unstable stationary nonlinear surface waves, exposing several exciting new phenomena such as nonlinear

* Corresponding author. Fax: +52-464-72400.
E-mail address: ealvarad@salamanca.ugto.mx (E. Alvarado-Méndez).

0030-4018/01/$ - see front matter © 2001 Published by Elsevier Science B.V.
PII: S0030-4018(01)01240-8

Goos–Hänchen effect and the transmission of self-focused channels (or solitons) through dielectric interfaces. Other important investigations were made by Aceves et al. [4–6]. Their theory addresses the propagation of self-focused channels in two or more nonlinear dielectric media. The nonlinear wave packet representing the self-focused channel is represented as an equivalent particle moving in an equivalent potential. The dynamics of the particle is described by Newton's equations of motion, with the asymptotic propagation paths of the channel being read off from the associated phase portraits of the equivalent potential. Subsequently, special cases of nonlinearity, have given rise to a broad variety of interesting phenomena. Among them, we can find filamentation [7], optical bistability [8], surface waves [9,10], etc. Furthermore, the proposed practical applications of these phenomena include controllable scanning beams [11], optical gates [12], weak beam amplification [13] and so on.

However, the problem of internal reflection of a bright spatial soliton in the interface nonlinear saturable-linear media has not been analyzed in detail. This problem may find practical applications when the spatial soliton acts as an optical wave guide for a weak beam of a different wavelength [14,15]. Some materials, for example, photorefractive crystals (PRC) exhibit saturable nonlinearity at very low powers, and in this paper we analyze, from the numerical and theoretical point of view, the behavior of a one-dimensional bright spatial soliton in a medium with saturable nonlinearity as it reaches the boundary with a linear medium. In particular, we are interested in determining the conditions under which a spatial soliton is obtained after reflection by the interface. Another important characteristic to conclude is if the incidence angle is conserved. The plan of present paper is as follows. In Section 2 we propose the mathematical model for the nonlinear saturable-linear interface. Since analytical solutions in nonlinear saturable mediums are unknown, we find stationary numerical solutions. These solutions are launched in a nonlinear interface with adequate parameter selection (angle of incidence, initial position of the beam, initial amplitude, etc.) and the total internal reflection is characterized. At the end of this section, we use Lagrangian approach to study if the reflected beam is soliton or not. In the last section, we present preliminary experimental results of total internal reflection of $(2+1)$D spatial soliton in photorefractive SBN61:Ce crystal. Finally, the conclusion of the work is presented.

2. Mathematical model for the nonlinear interface

Fig. 1 shows the geometry of the nonlinear interface of interest. The interfaces lies in the y–z plane at $x=0$, it separates a nonlinear medium with saturation on the left and a linear medium on the right. The nonlinear medium is characterized by a refractive index of the form [16,17],

$$n_1(I) = n_{01} + \eta \frac{\mu|a|^2}{1+\mu|a|^2} \tag{1}$$

where n_{01} is the linear refractive index, $\mu = I_{\text{sat}}/a_0^2$ is the saturation parameter, $a_0^2 = I_{\max}(0)$ is the intensity of the uniform background illumination. $\eta = L_{\text{D}}/L_{\text{NL}}$ or $\eta = n_{01}k_0x_0^2/(1/k_0\,\delta n_0)$, is the nonlinear coefficient of the medium, x_0 and a_0 are the width and initial amplitude respectively, $|a(x,z)|^2$ is the beam intensity, $\delta n_0 = (1/2)rn_{01}^3V_0/L$ is the nonlinear contribution to the refractive index, where r is the effective electro-optic coefficient, V_0 is the externally applied voltage, and L is the transverse width of the crystal. Eq. (1) describes a nonlinear saturable medium when drift mechanism is dominant [18,19] for the case of a slit beam. In the other hand, the linear medium (right side of Fig. 1) is characterized by a constant refractive index n_{02} with $n_{01} > n_{02}$. In Fig. 1 bright spatial soliton is depicted at the beginning of the nonlinear medium, the incidence (θ_{i}) and the reflection (θ_{r}) angles are also shown. The mathematical description of our problem is restricted to the case when a laser beam propagates in the positive direction of the z-axis, with linear polarization perpendicular to incident plane,

$$E_y = \tfrac{1}{2}a(x,z)\exp[\mathrm{i}(\omega t - k_2 z)] \tag{2}$$

where $a(x,z)$ is the slowly varying complex amplitude of the $(1+1)$D beam, ω is the carrier fre-

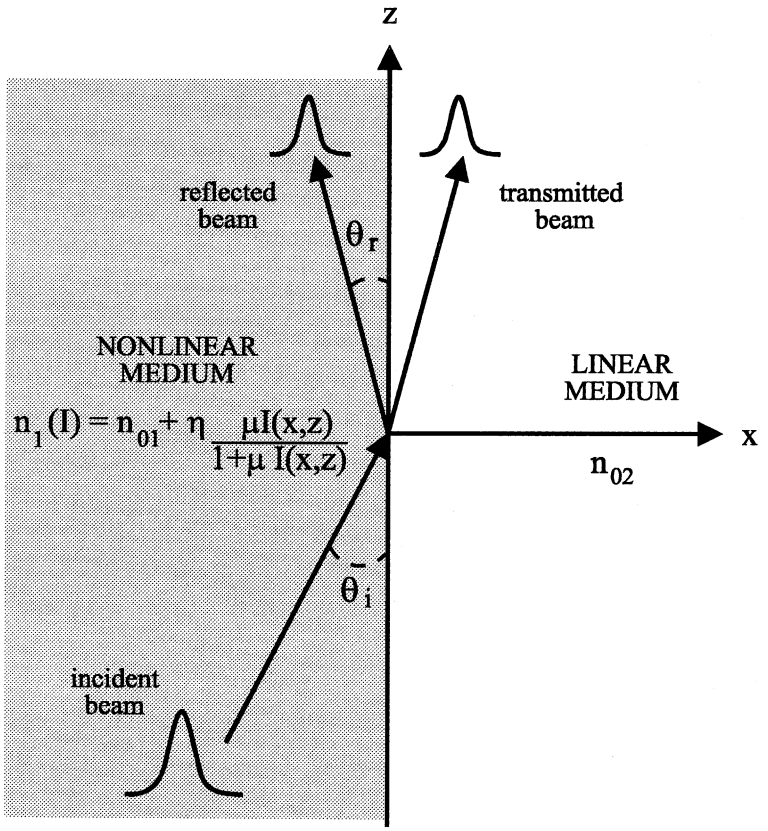

Fig. 1. A bright spatial soliton falling upon an interface between a saturable-like nonlinear and a linear media.

quency, and k_2 is the wave number. A valid approximation was assumed and that the complex amplitude satisfies the equation,

$$2ik_2\frac{\partial a}{\partial z}=\frac{1}{2}\frac{\partial^2 a}{\partial x^2}+k_2^2\frac{\delta n(x)}{n_{02}}a \tag{3}$$

where $\delta n(x)$ represents the nonlinear contribution to the refractive index. The refractive index profile of the two media at both sides of the nonlinear interface takes the form,

$$\delta n(x)=\left[(n_{01}-n_{02})+\eta\frac{\mu|a|^2}{1+\mu|a|^2}\right]f(x) \tag{4}$$

where $f(x)$ is a function which describes the spatial behavior of the interface. If the interface is abrupt, we considered a step function for $f(x)$; it means $f(x)=U(x)$, where $U(x)=1$ if $x\leqslant 0$, $U(x)=0$ for $x>0$. In computer simulation it is more convenient to use smooth function $f(x)=s(x)=1/2[1-\tanh(\kappa x)]$ to describe general interface, where κ represents the steepness of the interface. Notice that as κ increases $s(x)\to U(x)$.

If we substitute Eq. (4) into Eq. (3) we obtain,

$$i\frac{\partial a}{\partial Z}=\frac{1}{2}\frac{\partial^2 a}{\partial X^2}+\eta f(X)\left[\Delta+\frac{\mu|a|^2}{1+\mu|a|^2}\right]a \tag{5}$$

where $\Delta=(n_{01}-n_{02})/\tilde{n}_2|a_0|^2$ represents the normalized refractive index difference; $Z=z/L_d$ is the normalized propagation distance to the diffraction length $L_d=k_0n_{01}x_0^2$, $X=x/x_0$ is the transversal coordinate normalized to the initial beam width, the complex amplitude of the beam is normalized to the initial amplitude peak value.

Stationary solutions of Eq. (5) can be found by numerical techniques. We assume that the input

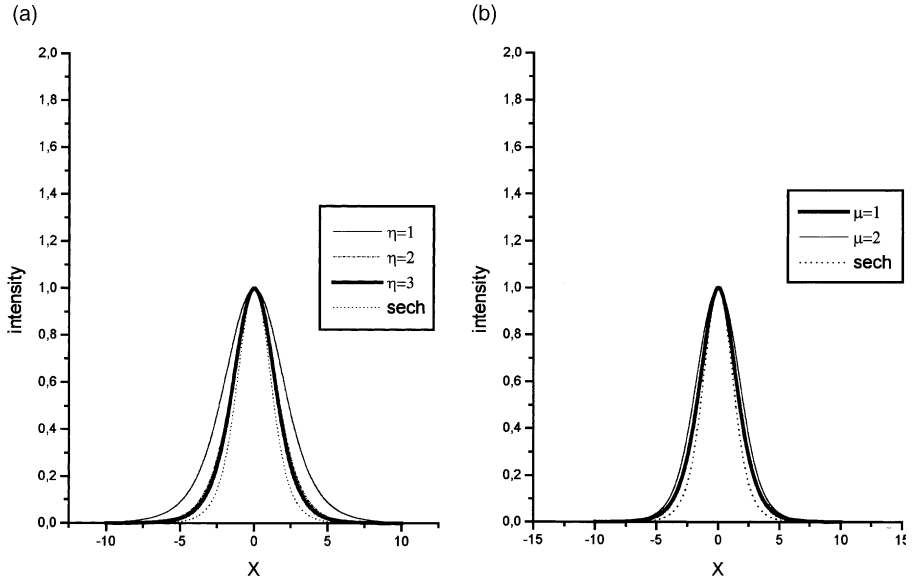

Fig. 2. Profiles of numerical solutions for different values of (a) saturation parameter, (b) saturation coefficient. The profiles are compared with a Kerr-like one.

soliton beam is far enough from the interface, with $f(X) = 1$ and $\Delta = 0$. If we using the standard ansatz,

$$a(X, Z) = \phi(X) \exp(-i\gamma Z) \tag{6}$$

Substituting the Eq. (6) into Eq. (5),

$$\frac{1}{2}\frac{d^2\phi}{dX^2} = \gamma\phi - \eta\frac{\mu|\phi|^2}{1+\mu|\phi|^2} \tag{7}$$

Eq. (7) is integrated numerically by the fourth order Runge–Kutta method for different parameters values (η, μ). In Fig. 2a the solution profiles are showed. If parameter μ increases, the beam width grows. The hyperbolic secant solution, that is valid for a Kerr-type medium, is also shown in this picture for comparison. In Fig. 2b the solutions are show when μ and ϕ are constants and parameter η is varied. In this case the profile width decreases and it is very close to the hyperbolic secant solution with numerical values of $\mu = 1$ and $\eta = 3$. So, for numerical simulation of the internal reflection of spatial soliton we used as initial condition. The numerical solution is,

$$a(x, 0) = a_{sol}(X - X_0, 0) \exp[-iV(X - X_0)] \tag{8}$$

where $a_{sol}(X - X_0, 0)$ is the numerical soliton solution, X_0 is the input beam center normalized coordinate, parameter V characterizes the incidence angle in normalized coordinates X, Z:

$$V = tg\theta_i = k_2 a_0 \tag{9}$$

3. Numerical simulations of total internal reflection of one spatial soliton

The Eq. (5) has been solved by conventional split-step numerical technique [20] with initial conditions given by Eq. (8). In computer simulation we used $f(X) = s(x)$, with $\kappa = 10$. This value has demonstrate be a good approximation for the steep nonlinear interface because for values of $\kappa > 10$ the result does not change significantly. Fig. 3 shows the total internal reflection of a spatial soliton. Notice that when a spatial soliton approaches the interface and is reflected, its peak intensity and width remains practically the same, proving that V parameter is small enough. In consequence, the energy is approximately conserved during the reflection at the nonlinear interface, this means that, the reflection of solitons may be called *elastic*.

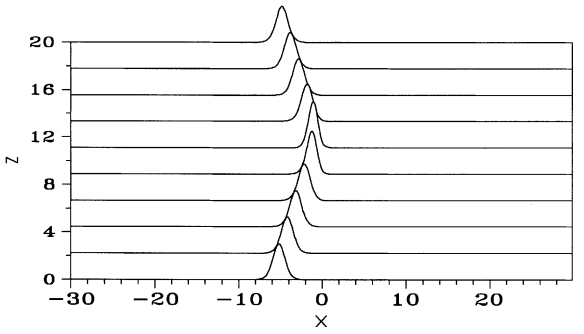

Fig. 3. Total internal reflection of the bright spatial soliton in saturable media, ($V_{in} < V_{cr}$). The numerical value of the incidence angle is $V = 0.5$, initial position $X_0 = 5$.

Fig. 4a shows the reflection of a spatial soliton with the incidence angle of $V = 1$. In this case the energy is splitted between reflected and transmitted beams. The beam transmitted to the linear medium spreads due to diffraction, while the beam reflected to the nonlinear medium conserves its soliton properties. Notice, that the width of the reflected soliton is bigger than that of the incident soliton due to the energy loss. This loss appears due to transmittance of high frequency components of the soliton spatial spectrum to the lineal medium. As a result the soliton spectrum is shifted to the low frequency region and the effective angle of reflection is decreased. In case of rather big incidence angle, the soliton is almost totally transmitted to the linear medium and diffracted ($V = 1.5$, Fig. 4b).

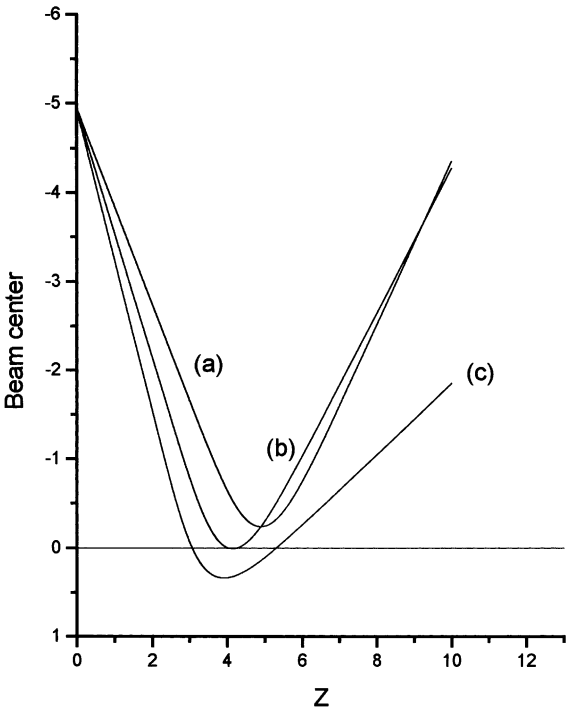

Fig. 5. Position of the beam center as a function of the propagation distance for several values of the incidence angle of the input spatial soliton (a) $V = 1.1$, (b) $V = 1.4$, (c) $V = 1.7$.

In Fig. 5 the position of the "integral" beam center as a function of the propagation distance for several values of the V parameter was plotted. The "integral" beam center is defined in the standard form,

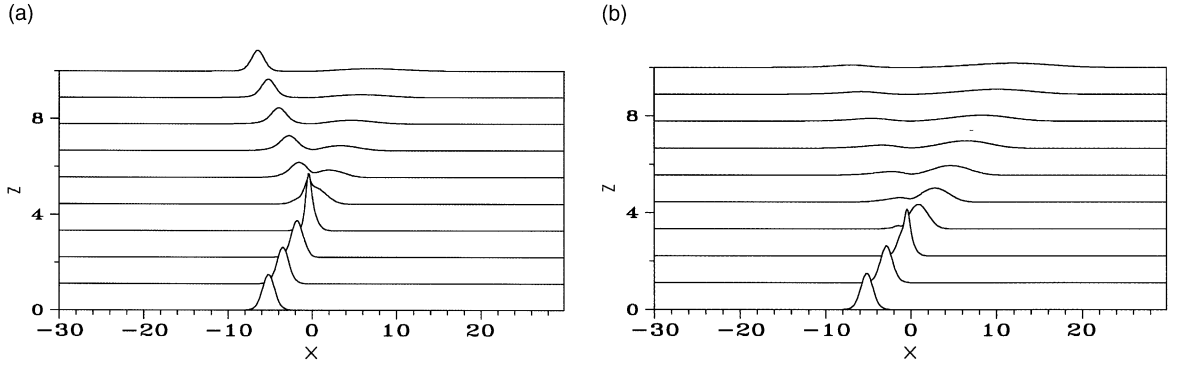

Fig. 4. Reflection and transmission of the bright spatial soliton for an initial incidence angle (a) $V = 1.7$ and (b) $V = 2.3$. The initial energy is splitted into the reflected and transmitted beams, but the reflected beam is still a spatial soliton.

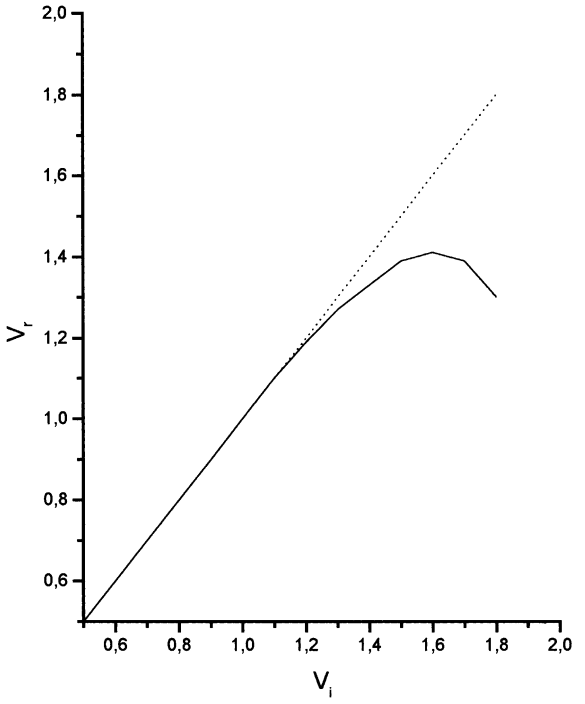

Fig. 6. The reflection angle as a function of the incidence angle.

$$\hat{x} \equiv \frac{\int_{-\infty}^{\infty} a^* X a \, \mathrm{d}X}{\int_{-\infty}^{\infty} a a^* \, \mathrm{d}X} \tag{10}$$

In case that the input beam splits between the two media, the reflected beam center, is calculated with a zero in the upper limit of the integral in Eq. (10). Fig. 5 one also can observe the dependence of the Goos–Hänchen shift and the penetration depth with the incident angle.

The unusual behavior of the angle of a spatial soliton reflection can be also observed in Fig. 6. When the absolute value of V_i parameter for the input soliton increases (in terms of collision it can be interpreted as the initial velocity growth) the resulting V_r parameter for the reflected soliton decreases due to the loss of momentum.

4. Variational approach

To be sure that the reflected beam is really a spatial soliton in a computer simulation, it is necessary to observe its behavior over a long propagation distance. Using the variational approach it is possible to establish the relation between the width and the amplitude of a soliton-like beam. The Lagrangian of the Eq. (5) is [21]:

$$L = \int \left\{ \frac{\mathrm{i}}{2}\left(a\frac{\partial a^*}{\partial Z} - a^*\frac{\partial q}{\partial Z}\right) - \frac{1}{2}\left|\frac{\partial a}{\partial X}\right|^2 + \eta|a|^2 - \frac{\eta}{\mu}\ln(1+\mu|a|^2)\right\} \mathrm{d}x \tag{11}$$

where X, y, Z are independent variables, a and a^* are dependent variables. The general Euler–Lagrange equation for m independent variables is [22],

$$\frac{\partial L}{\partial y_i} - \sum_{j=1}^{m} \frac{\partial}{\partial x_j}\left(\frac{\partial L}{\partial y_{ij}}\right) = 0 \tag{12}$$

with $i = 1, 2, \ldots$, $y_{ij} = \partial y_i/\partial x_j$; y_i as dependent variables, and x_j as independent variable.

We use the standard ansatz corresponding to a Gaussian beam,

$$a(X,Z) = A(Z)\exp\left(-\frac{(x-\bar{x}(Z))^2}{2\alpha^2(Z)}\right) \times \exp \mathrm{i}[(x-\bar{x}(Z))^2 b(Z) + \varphi(z)] \tag{13}$$

where $A(Z)$ is the real amplitude of the Gaussian beam, $\alpha(Z)$ is the beam width, $b(Z)$ is the parabolic phase front curvature, $\bar{x}(Z)$ is the coordinate of the beam center, and $\varphi(Z)$ is the phase shift. Further, suppose a stationary beams self-trapping in saturable media which propagate parallel to the Z-axis, $\bar{x}(Z) = 0$. Using the Eq. (13) in Eq. (11) we obtain the reduced Lagrangian,

$$\langle L\rangle = \alpha A^2\frac{\partial\varphi}{\partial z} + \eta\alpha A^2 - A^2\frac{1}{4\alpha} - b^2\alpha^3A^2 + \alpha^3\frac{1}{2}A^2\frac{\partial b}{\partial Z} - \frac{\eta}{\sqrt{\pi}\mu}\int_{-\infty}^{+\infty}\ln\left[1+\mu A^2\exp\left(-\frac{x^2}{\alpha^2}\right)\right]\mathrm{d}X \tag{14}$$

When the reduced Lagrangian is introduced into Eq. (12) analytical solutions do not exist, however if we simplify Eq. (14) assuming $\mu \ll 1$: $\ln[1+\mu A^2\exp(-x^2/\alpha^2)] \approx \mu A^2\exp(-x^2/\alpha^2)$, is pos-

sible to find an the variations of width α, amplitude A and the phase φ of a beam are,

$$\delta L_A = A\alpha^3 \frac{\partial b}{\partial Z} + 2\alpha A \frac{\partial \varphi}{\partial Z} - \frac{A}{2\alpha} - 2b^2 A\alpha^3 + 2A\alpha\eta - \frac{\eta}{\mu\sqrt{\pi}} \frac{\partial}{\partial A} \int \ln\left[1 + A^2\mu \exp(-x^2/\alpha^2)\right] \mathrm{d}x \tag{15}$$

$$\delta L_\alpha = A^2 \frac{3}{2}\alpha^2 \frac{\partial b}{\partial Z} + A^2 \frac{\partial \varphi}{\partial Z} + \frac{A^2}{4\alpha^2} - 3b^2 A^2\alpha^2 + \eta A^2 - \frac{\eta}{\mu\sqrt{\pi}} \frac{\partial}{\partial \alpha} \int \ln\left[1 + A^2\mu \exp(-x^2/\alpha^2)\right] \mathrm{d}x \tag{16}$$

$$\delta L_\varphi = -\frac{\partial}{\partial Z}(\sqrt{\pi} A^2 \alpha) = 0 \tag{17}$$

Notice that Eq. (17) is a consequence of beam energy conservation. It means that the power of the beam is constant along the propagation distance Z. To find a relation between the beam width and its amplitude, one can multiply the Eq. (17) by α, Eq. (16) by A, and add results finally obtaining:

$$4\alpha \frac{\partial b}{\partial Z} A^2 - \frac{\eta}{\mu\sqrt{\pi}} 3A \frac{\partial}{\partial A} \int \ln\left[1 + A^2\mu \exp(-x^2/\alpha^2)\right] \mathrm{d}x + 4\alpha\eta A^2 + \frac{1}{\mu\sqrt{\pi}} 2\alpha\eta \frac{\partial}{\partial \alpha} \int \ln\left[1 + A^2\mu \exp(-x^2/\alpha^2)\right] \mathrm{d}x - 2\frac{A^2}{\alpha} = 0 \tag{18}$$

Introducing a new variable $t = x/\alpha$ in Eq. (18), after some algebraic manipulation, it is possible to obtain information on the beam width variation as a function of the peak intensity in the form of equation:

$$\frac{1}{\alpha^2} = -\frac{4\eta}{\alpha\sqrt{\pi}} \int_0^\infty \left[\frac{\exp(-t^2)}{1 + \mu A^2 \exp(-t^2)}\right] \mathrm{d}t + \frac{8\eta}{\alpha\sqrt{\pi}} \int_0^{+\infty} \left[\frac{t^2 \exp(-t^2)}{1 + \mu A^2 \exp(-t^2)}\right] \mathrm{d}t \tag{19}$$

The relation between width (α) and intensity ($|A|^2$) is plotted in Fig. 7. Numerical solution of Eq. (5), is in good agreement with the behavior of the characteristic curve of Fig. 7. Furthermore, using this curve it is possible to determine if the reflected beam is a soliton or not.

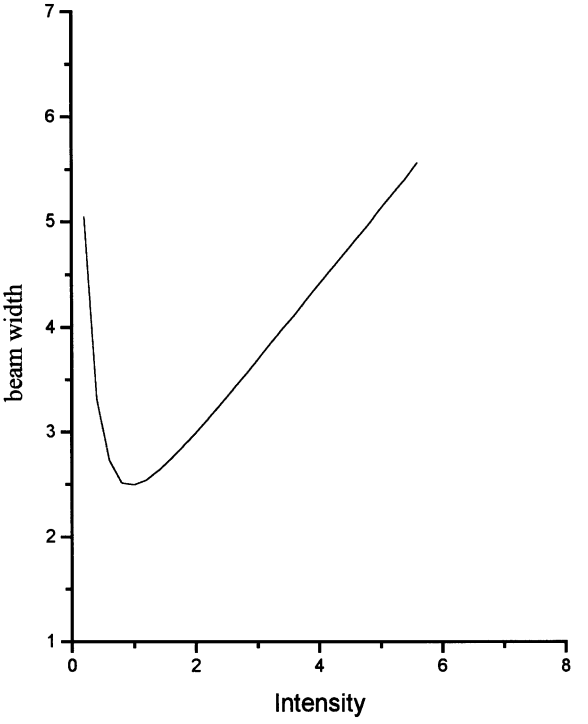

Fig. 7. Characteristic curve of the beam width as function of intensity. All the beams with parameters satisfying this curve are solitons.

5. Experimental results

In our experimental results a Gaussian beam is used for total internal reflection at an interface was formed by a nonlinear an linear media. SBN:61 crystal whit an electro-optic coefficient (r_{33}) 224 pm/V, refractive index 2.33, and 5 mm × 5 mm × 10 mm dimensions, is used as a nonlinear medium, the linear medium is air. The experimental setup is shown in Fig. 8, where a cw He–Ne laser *b* (632.8 nm, 10 mW power) is used to illuminate uniformly the PRC, the cw He–Ne laser *a* (632.8 nm, 20 mW power) is used to generate the Gaussian beam. A pair of mirrors are used to control the incident angle at the input face of the PRC. The output image is captured by CCD.

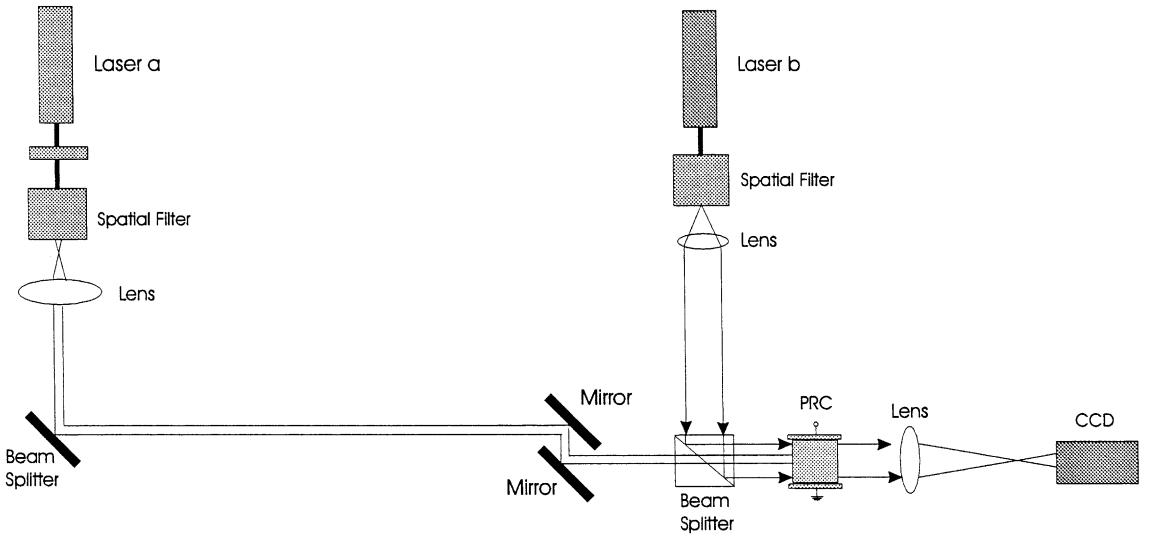

Fig. 8. Experimental setup.

Two cases can arise to analyze the properties of the incident beam, depending of the incident angle.

5.1. First case

Reflection and transmission: The width of the beam in the input face (1 1 0) was 35 μm and the angle between the incident beam and the normal of the input face was 2.57°. In this case, the initial beam (see Fig. 9a), after being reflected by the face (0 0 1) is splitted in two beams namely, one reflected and one transmitted without voltage applied as depicted in Fig. 9b. When 300 V/cm are applied to the crystal along of the face (1 1 1), the reflected beam is self-focused (see Fig. 9c) and the beam transmitted to the linear medium is diffracted. These effects correspond to numerical predictions previously explained in Section 3 (see Fig. 4a).

5.2. Second case

Total internal reflection: The width of the beam is the same and the angle between the incident beam and the normal of the input face was 1.25°. The initial beam (see Fig. 10a) is reflected totally by the face (0 0 1) without voltage applied as depicted in Fig. 10b. When 600 V/cm are applied to the face (1 1 1) and after 20 s, the reflected beam is self-focused as shown in Fig. 10c. This corresponds to the case of total internal reflection previously explained in Section 3 (see Fig. 3).

The results presented in Fig. 10c, are in good qualitative agreement with the general behavior of the spatial solitons – a stronger nonlinearity can give place to (i.e. the higher value of the dc voltage applied) narrower beams.

This preliminary experimental results can be considered satisfactory and corroborate the numerical and theoretical predictions about the physical conditions to generate self-focused beams in total internal reflection.

6. Conclusions

Total internal reflection of spatial soliton at a nonlinear interface, which divides a saturable-like and a linear medium was studied. This study was focused on the possibility to obtain a reflected spatial soliton. Our results show that there are three fundamental cases:

(i) if $V_{in} < V_{cr}$, we have total internal reflection. (ii) if $V_{in} \leqslant V_{cr}$, the soliton is reflected and transmitted and, if the reflected beam correspond to

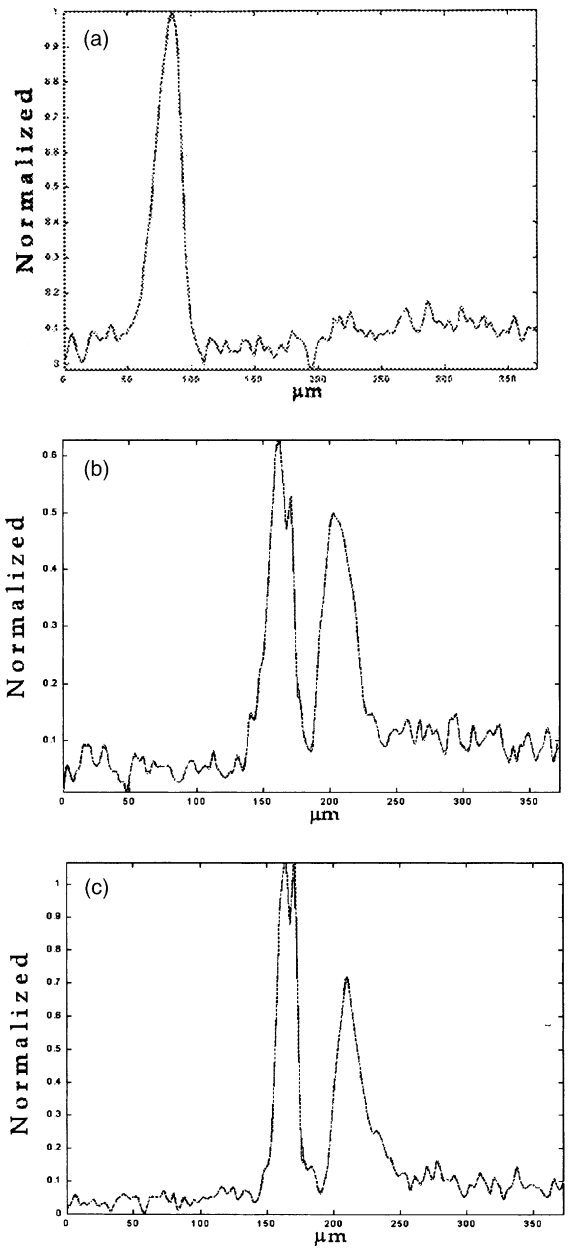

Fig. 9. Transverse profile for one beam transmitted and reflected on the (a) input face crystal, (b) output face crystal without voltage, (c) output face crystal with 300 V.

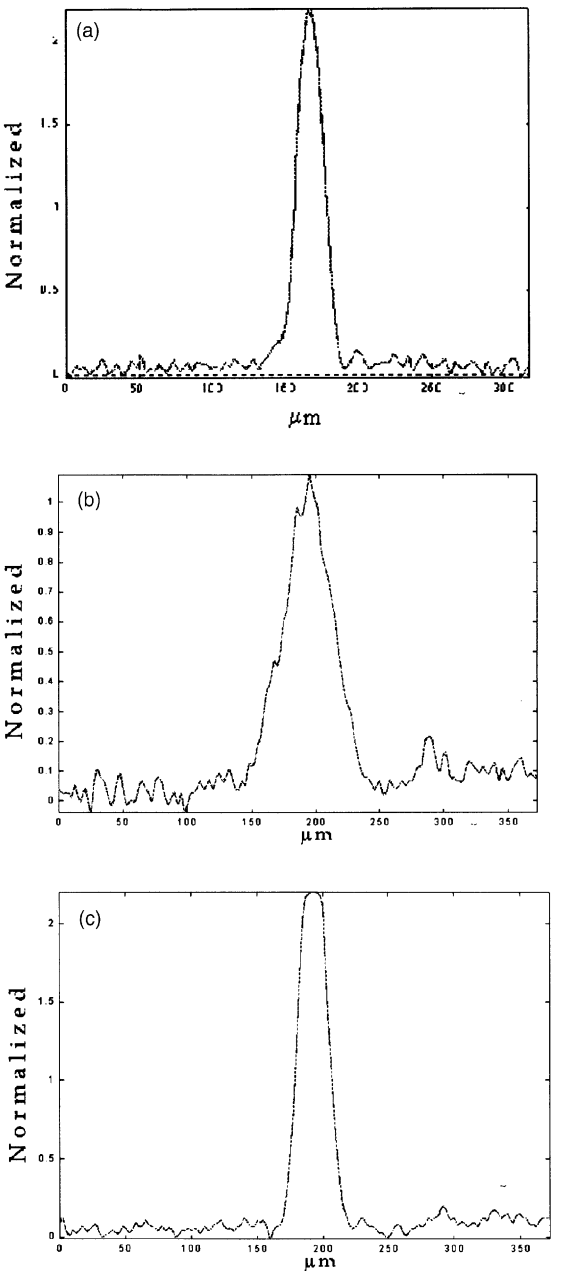

Fig. 10. Total internal reflection of one beam for (a) input face, (b) output face crystal without voltage, (c) output face crystal with 600 V.

characteristic curve (Fig. 7), then it is a soliton. In this region the reflected soliton is affected by a Goos–Hänchen shift. Finally, (iii) for large input angles $V_{in} \gg V_{cr}$, a large part of the input energy is transmitted to the second medium in the form of a spreading beam. In this case, the reflected beam does not form a spatial soliton.

Experimentally we obtained total internal reflection of spatial solitons in a SBN61:Ce PRC. The results are in close agreement with the numerical simulations.

Acknowledgements

This work was supported by CONACyT, projects 27307-E and J32018-A. In memory of our friend Gustavo E. Torres-Cisneros.

References

[1] A.E. Kaplan, JETP Lett. 24 (1976) 115.
[2] A.E. Kaplan, Sov. Phys. JETP 45 (1997) 896.
[3] N.N. Akhmediev, V.I. Korneev, Yu.V. Kuz'menko, Sov. Phys. JETP 61 (1985) 62.
[4] A.B. Aceves, J.V. Moloney, A.C. Newell, Phys. Rev. A 39 (1989) 1809.
[5] A.B. Aceves, J.V. Moloney, A.C. Newell, Phys. Rev. A 39 (1989) 1828.
[6] A.B. Aceves, J.V. Moloney, A.C. Newell, Opt. Lett. 13 (1988) 1002.
[7] W.J. Tomlinson, J.P. Gordon, P.W. Smith, A.E. Kaplan, Appl. Opt. 21 (1982) 2041.
[8] P.W. Smith, W.J. Tomlinson, P.J. Maloner, J.P. Hermann, IEEE J. Quant. Electron. QE-17 (1984) 340.
[9] H.T. Tran, J. Nonlinear Opt. Phys. Mat. 5 (1996) 133.
[10] G.S. García-Quirino, J.J. Sánchez-Mondragón, S. Stepanov, Phys. Rev. A 51 (1995) 1571.
[11] A.B. Aceves, P. Varatharajah, A.C. Newell, E.M. Wright, G.I. Stegeman, D.R. Heatley, J.V. Moloney, H. Adachihara, J. Opt. Soc. Am. B 7 (1990) 963.
[12] P.W. Smith, W.J. Tomlinson, IEEE J. Quant. Electron. QE-20 (1984) 30.
[13] A.V. Khomenko, A. García-Weidner, A.A. Kamshilin, Opt. Lett. 21 (1996) 1014.
[14] M. Segev, G.C. Valley, B. Crosigniani, P. Di Porto, A. Yariv, Phys. Rev. Lett. 73 (1994) 3211.
[15] M.D. Iturbe-Castillo, J.J. Sánchez-Mondragón, V.A. Vysloukh, S.I. Stepanov, S. Chávez-Cerda, G.E. Torres-Cisneros, Opt. Lett. 20 (1995) 1853.
[16] P.J. Bradley, C. De Angelis, Opt. Commun. 130 (1996) 205.
[17] V.E. Wood, E.D. Evans, R.P. Kenan, Opt. Commun. 69 (1988) 156.
[18] P. Roussignol, D. Ricard, J. Lukasik, C. Flytzanis, J. Opt. Soc. Am. B 4 (1987) 5.
[19] L.H. Acioli, A.S.L. Gomes, J.M. Hickman, C.B. deAraujo, Appl. Phys. Lett. 56 (1990) 2279.
[20] G.P. Agrawall, Nonlinear Fiber Optics, Academic Press, New York, 1989, p. 44.
[21] O. Cornejo Vázquez, Fuezas de interacción entre dos haces unidimensionales Gausianos en un cristal fotorrefractivo, Master Thesis, Universidad de Guanajuato (FIMEE), Octubre de 1997.
[22] V.M. Agranovich, V.S. Babichenko, V.Ya. Chernyac, Sov. Phys. JETP Lett. 32 (1980) 512.